

# HAZE AND SMOKE REMOVAL FOR VISUALIZATION OF MULTISPECTRAL IMAGES: A DNN PHYSICS AWARE ARCHITECTURE

*Iulia Coca Neagoe<sup>1</sup>, Corina Vaduva<sup>1</sup>, Mihai Datcu<sup>1,2</sup>*

<sup>1</sup> Research Center for Spatial Information (CEOSpaceTech), University POLITEHNICA of Bucharest (UPB)

<sup>2</sup> Earth Observation Center (EOC), German Aerospace Center (DLR)

## ABSTRACT

Remote sensing multispectral images are extensively used by applications in various fields. The degradation generated by haze or smoke negatively influences the visual analysis of the represented scene. In this paper, a deep neural network based method is proposed to address the visualization improvement of hazy and smoky images. The method is able to entirely exploit the information contained by all spectral bands, especially by the SWIR bands, which are usually not contaminated by haze or smoke. A dimensionality reduction of the spectral signatures or angular signatures is rapidly obtained by using a stacked autoencoders (SAE) trained based on contaminated images only. The latent characteristics obtained by the encoder are mapped to the R – G – B channels for visualization. The haze and smoke removal results of several Sentinel 2 scenes present an increased contrast and show the haze hidden areas from the initial natural color images.

**Index Terms**— Remote sensing, multispectral, haze and smoke removal, autoencoder, data visualization.

## 1. INTRODUCTION

Optical satellite images are a measurement of the light reflected by the earth surface. The presence of water vapor, ice, fog, smoke or other particles in the atmosphere generates light scattering in the process of propagation. The consequences of this process comprise low contrast, blurred surface colors and even hidden areas behind high amplitude pixel values. Many visual analysis applications, including change detection mapping, disaster monitoring or climate change monitoring are affected, therefore an effective contamination removal method is of great importance. The purpose of haze removal is to eliminate the distortion factor from the image. Usually, cloudy images do not contain any information about the ground surface, but images affected by smoke and fog still contain important spectral information. The haze transparency offers a valuable opportunity to decontaminate and restore images.

During the past years, numerous remote sensing single image haze removal methods have been studied and

proposed based on various prior information and assumptions. An atmospheric scattering correction technique for optical data based on dark object subtraction (DOS) was presented by Chavez [1], [2]. Zhang et al. [3] propose a haze optimized transformation (HOT) for the characterization of spatial distribution of haze and the false HOT responses generated numerous strategies research and approaches [4], [5], [6], [7]. Among the haze removal techniques literature presents the ones based on background suppressed haze thickness index (BSHTI) [8], haze thickness map (HTM) [9], [10] and a homomorphic filter [11], [12].

Dark channel prior (DCP) discovered by He et al. [13] represents an effective method of haze removal in computer vision. Due to its success on natural images, it gained attention in the remote sensing field and numerous DCP based methods were developed [14], [15], [16]. Although on multimedia images proves to be very adequate, on remote sensing images its success is limited by the wide ground surface covered by one scene.

Recently, machine learning based methods were developed to remove haze from images. For the estimation of haze transmission Tang et al. [17] combined haze relevant features. Cai et al. [18] proposed DehazeNet, a convolutional neural network (CNN) based method to estimate haze transmission. DehazeNet proves to be superior over existing methods regarding performance on multimedia images but for remote sensing images encounters spatial variability problems. Following the great achievements of CNNs for image processing, Jiang et al. [19] and Qin et al. [20], proposed multi-scale CNNs with residual architecture to remove haze from multispectral images. Both methods use only the visible and near-infrared bands of Landsat 8 Operational Land Imager (OLI). However, to the best of our knowledge, an autoencoder network has not been proposed for dehazing multispectral remote sensing images.

In this paper, we propose a stacked autoencoder(SAE) to remove haze and smoke from the visualization of a single multispectral image by using the information from short-wave infrared (SWIR) bands. Previously, we also proposed a visualization method in [21] which improved contrast and eliminated similarities and dissimilarities ambiguities. The

visualization obtained resulted from the translation of the encoder output latent features to the R – G – B channels.

We take a step forward and translate the data from color feature to angular distances space representation. To this aim, we use the illumination invariant features through the polar coordinate transformation of the reflectance values in two different scenarios:

- 1) The angular signatures are provided as input to the network and the autoencoder is trained to reconstruct the input;
- 2) The network receives as input the spectral signatures and loss during training is evaluated by comparing the angular signatures of the input with the angular signatures of the decoder output.

Both scenarios imply training on hazy and smoky images without the need of clear images. The proposed method aims to improve color contrast of visualized scene, rapidly remove smoke and haze without intensive computation and make use of unlabeled data. Evaluation is performed on Sentinel 2 Level 2A processed hazy images.

## 2. ILLUMINATION INVARIANT FEATURES

In the context of haze removal from remote sensing images, the polar coordinates transformation provides a suitable solution to obtain illumination invariant features. Georgescu et al. [22] proposed a descriptor based on polar coordinates transformation. The polar feature space created can be used for the computation if the MPEG-7 scalable color descriptor. An enhanced optical images analysis using polar coordinates was first introduced by Okamura et al. [23]. As far as it goes, the use of illumination invariant descriptor it has been proven to be very useful for contaminated multispectral remote sensing images.

The radiances values of the spectral bands are translated into polar coordinates. The image is characterized by a distance  $\rho$  and  $N-1$  angles  $\theta$ ,  $N$  representing the number of spectral bands. The following transformations are performed in order to represent the image by use of  $\rho$  and  $\theta$ .

$$\rho = \sqrt{x_N^2 + x_{N-1}^2 + \dots + x_2^2 + x_1^2} \quad (1)$$

$$\theta_1 = \arctan \frac{\sqrt{x_N^2 + x_{N-1}^2 + \dots + x_2^2}}{x_1} \quad (2)$$

$$\theta_2 = \arctan \frac{\sqrt{x_N^2 + x_{N-1}^2 + \dots + x_3^2}}{x_2} \quad (3)$$

$$\theta_{N-2} = \arctan \frac{\dots}{x_{N-2}} \quad (4)$$

$$\theta_{N-1} = 2 \arctan \frac{x_N}{x_{N-1} + \sqrt{x_N^2 + x_{N-1}^2}} \quad (5)$$

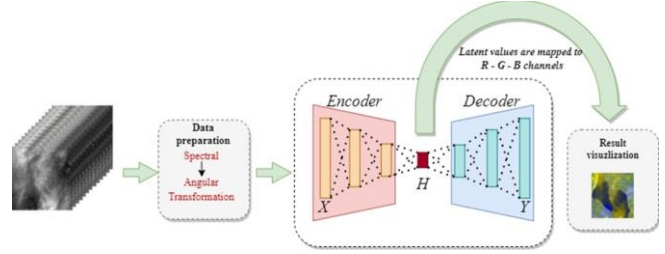


Fig. 1 Architecture of the SAE network proposed for haze and smoke removal from multispectral images; we present two scenarios, *first* – the network receives as input the angular signatures and *second* – the network receives as input spectral signatures, but the optimization is computed using angular signatures

where  $x_1, x_2, \dots, x_N$  represent the radiance values of each band  $i, i=1 \dots N$ . The number of resulted polar features equals the number of spectral features from the multispectral image.

## 3. HAZE AND SMOKE REMOVAL METHOD

Being often used for embedding tasks, neural networks like autoencoders, learn as much information as possible of the input dataset. Their lower dimensionality and the unsupervised way of learning represent the main advantages of this type of neural networks.

The architecture of autoencoders consists of a two modules: encoder and decoder. The first one compresses an input,  $X$ , and has as result a hidden representation,  $H$ , at the bottleneck layer. The second one receives as an input the representation  $H$  and tries to compute the inverse transformation in order to reconstruct  $X$ . The result of the decoder,  $Y$ , represents the output of the network and it is supposed to be as similar as possible to  $X$ .

Our proposed method aims to improve visualization of hazy and smoky multispectral images by making use of the information from all spectral bands, in particular of the SWIR band. As it is shown in Fig. 1, we use the spectral bands as starting point in our network, then with the latent representation obtained by the embedding process generate a pseudo-color representation by mapping the three hidden values to R – G – B channels.

Following two different scenarios, the architecture of the network is not changed in terms of dimensions of inputs, latent representation, outputs and number of hidden layers.

First scenario implies an angular signature vector as input, the autoencoder having as purpose the reconstruction of these illumination invariant features. The loss function is computed by the minimization of mean squared error (MSE) between input and decoder result.

The second scenario uses the radiance values of the spectral bands as input and it has a loss function which minimizes the MSE between angular signatures of input and angular signatures of the decoder result.

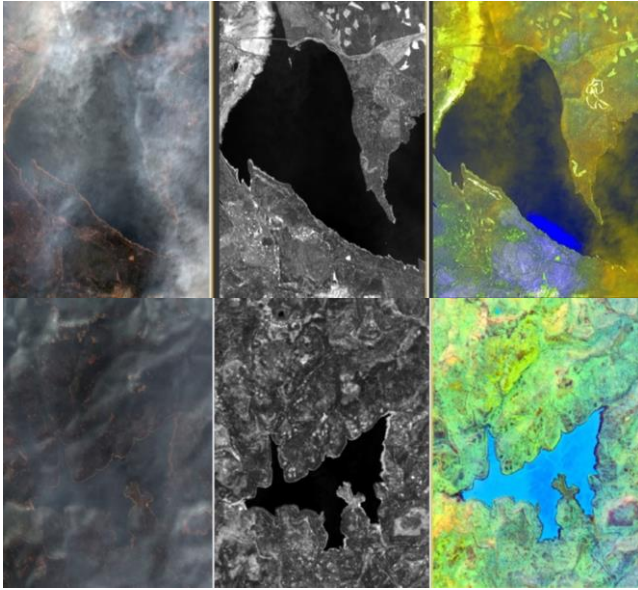


Fig. 2 Visualization comparison between true color representation, band B11 (SWIR) of the multispectral image and the result of SAE mapped to R - G - B channels; SAE takes as input angular signatures.

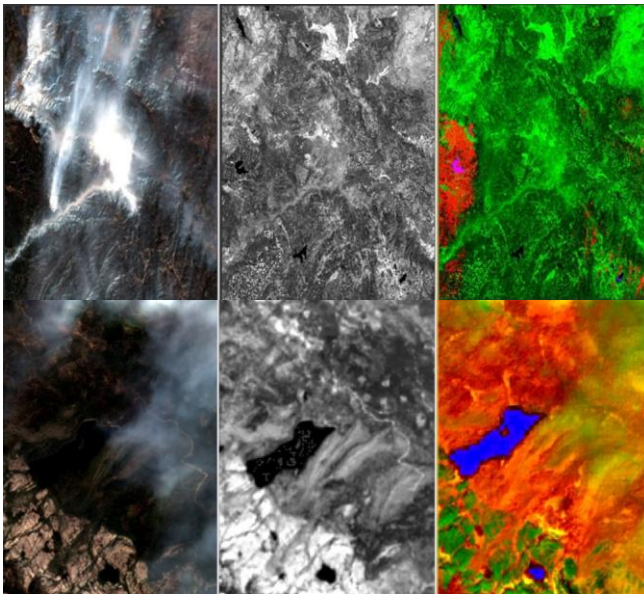


Fig. 3 Visualization comparison between true color representation, band B11 (SWIR) of the multispectral image and the result of SAE mapped to R - G - B channels; SAE takes as input angular signatures.

## 4. EXPERIMENTAL RESULTS

### 1. Experimental setup

Sentinel 2 processed at Level 2A products over Sacramento, California during ongoing fires were used for the experimental part of the paper. Level 2 processed products

do not contain band 10 because it does not include information about the surface, so the products have only 12 bands.

The architecture on the SAE consists of 7 fully connected hidden layers, with the following topology “10-8-6-3-6-8-10”. The bottleneck layer generates an output with three latent values which are used for the mapping to the R – G – B representation.

The training dataset consisted of a whole Sentinel 2 scene of 10980x10980x12 values. Before starting training we processed this matrix by scaling it using min-max normalization and resizing it obtaining a matrix  $(R * C) * B$ , where  $R$  represents the number of rows,  $C$  is the number of columns and  $B$  is the number of bands.

Having two scenarios, although the general architecture of SAE was the same, the parameters like learning rate, number of epochs and batch dimension were different. The first scenario implied a 150 epochs, the dimension of batches was 10980 and learning rate was set to 0.001. The second scenario involved a training process during 100 epochs with batches of 10980x2 and learning rate 0.0001. All of these parameters values were set experimentally, after testing the results of different setups.

### 2. Experimental results presentation

The visualization of multispectral remote sensing images affected by smoke does not provide much information about the earth's surface if done using the conventional method of mapping the bands from the visible part of the spectrum on R – G – B channels. Consequently, using a method that encompasses information from all spectral bands could be more useful.

Fig. 2 emphasizes the fact that SAE preserves the whole information from all spectral bands, but makes use of the important information from the SWIR band (B11). The two examples show an area with water bodies to emphasize the contrast and structures hidden under the smoke. Although SAE result shows a part of the smoke, the contour of the objects on ground is precise, like in the B11 representation. On the other hand, the visualization of the water body using true color representation is hampered by smoke.

Fig. 3 represents a comparison between a true color representation, B11 grey representation and the latent values obtained by an intermediate second scenario of SAE mapped to R – G – B channels. This second scenario uses the spectral signatures as input to the network, while the angular distances are used for the computation of loss error. The visualization is definitely improved and the contrast is elevated. The first example of this scenario shows a very dense smoke area which in SWIR band 11 visualization is no longer present. The second example reveals a water body which is not visible in the real color representation and also demonstrates the improvement regarding contrast.

Although resulted visualization still shows part of the haze or smoke, the hidden areas become visible too and the contrast highlights the real ground aspect and objects.

## 5. CONCLUSIONS

In this paper, a deep neural network based method is proposed to address the visualization improvement of hazy and smoky images. The method accomplishes to make use of all information contained by all spectral bands, especially by the SWIR bands, which usually are not contaminated by haze or smoke. A dimensionality reduction of the spectral signatures or angular signatures is rapidly obtained by stacked autoencoders (SAE) trained using only contaminated images. The latent characteristics obtained by the encoder are mapped to the R – G – B channels for visualization. The haze and smoke removal results of several Sentinel 2 scenes present an increased contrast and show the haze hidden areas from the initial natural color images.

The proposed method visualization succeeds to show hidden areas by using the existent spectral information and does not imply any synthetic transformation.

## 6. ACKNOWLEDGMENT

Part of this work was supported by a grant of the Romanian Ministry of Education and Research, CNCS-UEFISCDI, project number PN-III-P4-ID-PCE-2020-2120, within PNCIDI III.

## 7. REFERENCES

- [1] P.S. Chavez, "An improved dark-object subtraction technique for atmospheric scattering correction of multispectral data." *Remote sensing of environment*, 24(3), pp. 459-479, April 1988.
- [2] P.S. Chavez, "Image-based atmospheric corrections-revisited and improved." *Photogrammetric engineering and remote sensing*, 62(9), pp. 1025-1035, September 1996.
- [3] Y. Zhang, B. Guindon, and J. Cihlar, "An image transform to characterize and compensate for spatial variations in thin cloud contamination of Landsat images", *Remote Sensing of Environment*, 82(2-3), pp. 173-187, October 2002.
- [4] X. Y. He, J. B. Hu, W. Chen and X. Y. Li, "Haze removal based on advanced haze-optimized transformation (AHOT) for multispectral imagery", *International Journal of Remote Sensing*, 31(20), pp. 5331-5348, October 2010.
- [5] H. Jiang, N. Lu and L. Yao, "A high-fidelity haze removal method based on hot for visible remote sensing images", *Remote Sensing*, 8(10), pp. 844, October 2016.
- [6] S. Chen, X. Chen, J. Chen, P. Jia, X. Cao and C. Liu, "An iterative haze optimized transformation for automatic cloud/haze detection of Landsat imagery", *IEEE Transactions on Geoscience and Remote Sensing*, 54(5), pp. 2682-2694, December 2015.
- [7] L. Sun, R. Latifovic, and D. Pouliot, "Haze removal based on a fully automated and improved haze optimized transformation for Landsat imagery over land", *Remote Sensing*, 9(10), pp. 972, September 2017.
- [8] C. Liu, J. Hu, Y. Lin, S. Wu and W. Huang, "Haze detection, perfection and removal for high spatial resolution satellite imagery", *International Journal of Remote Sensing*, 32(23), pp. 8685-8697, August 2011.
- [9] A. Makarau, R. Richter, R. Müller and P. Reinartz, "Haze detection and removal in remotely sensed multispectral imagery", *IEEE Transactions on Geoscience and Remote Sensing*, 52(9), pp. 5895-5905, September 2014.
- [10] A. Makarau, R. Richter, D. Schläpfer and P. Reinartz, "Combined haze and cirrus removal for multispectral imagery", *IEEE Geoscience and Remote Sensing Letters*, 13(3), pp. 379-383, March 2016.
- [11] H. Shen, H. Li, Y. Qian, L. Zhang and Q. Yuan, "An effective thin cloud removal procedure for visible remote sensing images", *ISPRS Journal of Photogrammetry and Remote Sensing*, 96, pp. 224-235, October 2014.
- [12] O. R. Mitchell, E. J. Delp and P. L. Chen, "Filtering to remove cloud cover in satellite imagery", *IEEE Transactions on Geoscience Electronics*, 15(3), pp. 137-141, July 1977
- [13] K. He, J. Sun, and X. Tang, "Single image haze removal using dark channel prior," *IEEE transactions on pattern analysis and machine intelligence*, vol. 33, pp. 2341-2353, December 2011
- [14] J. Long, Z. Shi, W. Tang, and C. Zhang, "Single remote sensing image dehazing", *IEEE Geoscience and Remote Sensing Letters*, vol. 11, pp. 59-63, 2014.
- [15] X. Pan, F. Xie, Z. Jiang and J. Yin, "Haze removal for a single remote sensing image based on deformed haze imaging model", *IEEE Signal Processing Letters*, 22(10), pp. 1806-1810, 2015.
- [16] H. Jiang, N. Lu, L. Yao and X. Zhang, "Single image dehazing for visible remote sensing based on tagged haze thickness maps", *Remote Sensing Letters*, 9(7), pp. 627-635, 2018.
- [17] K. Tang, J. Yang and J. Wang, "Investigating haze-relevant features in a learning framework for image dehazing", In *Proceedings of the IEEE conference on computer vision and pattern recognition*, Beijing, China, pp. 2995-3000, June 2014.
- [18] B. Cai, X. Xu, K. Jia, C. Qing, and D. Tao, "Dehazenet: An end-to-end system for single image haze removal," *IEEE Trans. Image Process.*, vol. 25, no. 11, pp. 5187-5198, November 2016
- [19] H. Jiang and N. Lu, "Multi-scale residual convolutional neural network for haze removal of remote sensing images", *Remote Sensing*, 10(6), pp. 945, June 2018.
- [20] M. Qin, F. Xie, W. Li, Z. Shi and H. Zhang, "Dehazing for multispectral remote sensing images based on a convolutional neural network with the residual architecture", *IEEE Journal of Selected Topics in Applied Earth Observations and Remote Sensing*, 11(5), pp. 1645-1655, May 2018.
- [21] I. Neagoe, D. Faur, C. Vaduva and M. Datcu, "Exploratory Visual Analysis of Multispectral EO Images Based on DNN," *IEEE International Geoscience and Remote Sensing Symposium*, Valencia, pp. 2079-2082, July 2018.
- [22] F. A. Georgescu, D. Răducanu and M. Datcu, "New MPEG-7 scalable color descriptor based on polar coordinates for multispectral earth observation image analysis", *IEEE Geoscience and Remote Sensing Letters*, 14(7), pp. 987-991, July 2017.
- [23] T. Okamura, J.-I. Kudo, and K. Tanikawa, "Multispectral illumination invariant classification with three visible bands and a near-infrared band," *Opt. Eng.*, vol. 42, no. 6, pp. 1665-1672, 2003